Development of Cerium-based Conversion Coating on AZ31 Magnesium Alloy

S. A. Salman,* Ryoichi Ichino, and Masazumi Okido
*Department of Materials Science and Engineering, Graduate School of Engineering,
Nagoya University, Furo-cho, Chikusa-ku, Nagoya 464-8603*

The use of chromate baths is being progressively restricted owing to the high toxicity of the hexavalent chromium (Cr^{6+}) compounds. In this work, chemical conversion coating on AZ31 (3% Al, 1% Zn) magnesium alloy was performed by immersion in 5 mM $Ce(NO_3)_3$ solution with and without addition of $Al(NO_3)_3$ and $Ca(OH)_2$. It was noted that addition of $Al(NO_3)_3$ and $Ca(OH)_2$ to the cerium-based solution enhanced the surface properties and the corrosion resistance from anodic polarization in a 0.017 mol/L NaCl and 0.1 mol/L Na_2SO_4 solution at 298 K.

The importance of magnesium alloys in various industries has increased significantly because of the high strength/weight ratio, high dimensional stability, good machining, and ability to be recycled.[1,2] However, surface treatments are necessary in order to protect against corrosion and to achieve the resistance necessary for many applications. Commonly applied surface treatment is the chemical conversion in which chromate bath was traditionally applied in spite of being not friendly to the environment. It is toxic to human and difficult to be recyclable.[4,5]

Alternative surface treatments are needed. One of the most promising systems is based on rare earth elements. The solution is considered to be friendly to the environment. Therefore, several researchers have demonstrated that treatments with cerium-based aqueous solution effectively inhibited corrosion and affect the formation and properties of the conversion coatings.[5,9] The addition of aluminum compounds to the solution further improves the cerium treatments of the magnesium alloy.[10]

It has been reported that the addition of Ca to magnesium alloy improves the mechanical properties and the oxidation behavior of the alloy.[11,12]

Herein, we examine the effects of $Ca(OH)_2$ and $Al(NO_3)_3$ additives to cerium-based solution on the morphology and corrosion resistance of the cerium conversion layer.

Commercially available AZ31 Mg alloy (3 mass % Al, 1 mass % Zn) was used as the substrate. After the surface of the alloy was polished up to the # 2000 emery paper followed by 0.05 μm alumina powder,[9] the specimens were carefully cleaned with water, rinsed with acetone and dried under air. The specimens were mounted using PTFE resin tape, leaving 1 cm² surface area.

The cerium conversion coating was obtained by immersion of the specimens in the following three solutions: (1) 5 mM $Ce(NO_3)_3$ (pH 4.5), (2) 5 mM $Ce(NO_3)_3$ + 1 mM $Ca(OH)_2$ (pH 6.5) and (3) 5 mM $Ce(NO_3)_3$ + 1.5 mM $Al(NO_3)_3$ + 1 mM $Ca(OH)_2$ (pH 4.7).

The conversion coating time was 15 min, and the solution was agitated using a magnetic stirrer throughout the immersion. Scanning electron microscopy (SEM) was performed using a Hitachi S-800 to investigate the surface morphology and cross section of the conversion coating film. The chemical composition and phase structure of the conversion coating were determined via en-ergy-dispersive spectrometry (EDS) and X-ray diffraction (XRD). In order to characterize the corrosion properties of the chemical conversion treatment film, the potentiodynamic polarization tests were carried out at 298 K using a Solartron 1285 potentiostat with a scan rate 1 mV/s in a 17 mM NaCl and 0.1 M Na_2SO_4 solution at 298 K. A three-electrode cell with the coated specimens as the working electrode, Ag/AgCl/sat KCl as the reference electrode, and a platinum coil as a counter electrode, was used in the tests.

The nontreated specimen as indicated by SEM analysis contained polishing scratch shown in Figure 1(1). After 5 min conversion coating, the surface of specimen was partly covered by particles aligned themselves in rows along the scratch marks induced during mechanical polishing, indicating that the coating film was still very thin (Figure 1(2)). After 10 min, the thickness of the film increased and the coating was thick enough to cover the whole surface (Figure 1(3)). Several cracks were observed after 15 min immersion (Figure 1(4)). Possibly the cracks are formed during the drying of the specimen. The evaporation of water molecules caused shrinkage in the coated film and this could not happened in the thin coating because of the low amount of water molecules. At the early stages of immersion, the mass gain increased significantly from 2 to 10 min of immersion time. Then, the mass gain increased at a constant low rate during the last period; 10 to 15 min. the corrosion rate was evaluated from the polarization curves, Increasing of the immersion time enhanced the anticorrosion property, and the best corrosion resistance is observed at 15 min in this experiment (the figures not shown in this paper).

Figures 2a and 2b show the surface morphology and cross section of the coated films on AZ31 magnesium alloy after conversion coating in cerium-based solution with and without addition of $Al(NO_3)_3$ and $Ca(OH)_2$. After treatment in 5 mM $Ce(NO_3)_3$ solution, the coating film covers the surface of the substrate completely, with some microcracks visible in the SEM image as shown in Figure 2a(1). The cross section of this coating contained some microcracks as shown in Figure 2b(1). With
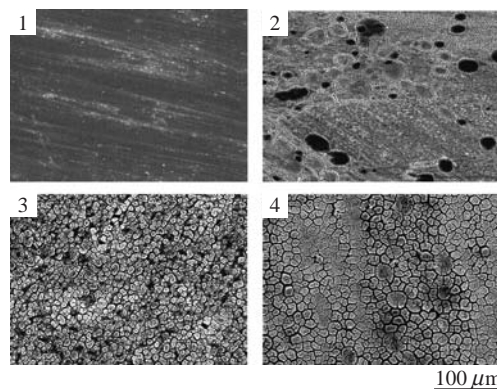
Figure 1. Surface morphology before (1) and after treatment in 0.05 M $Ce(NO_3)_3$ for (2) 5, (3) 10, and (4) 15 min.
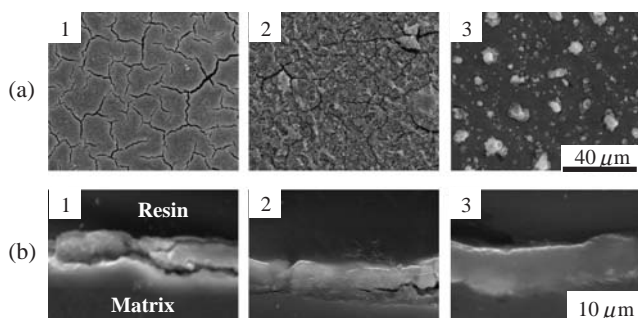
**Figure 2.** Surface morphology (a) and cross section (b) after 15 min treatment in (1) 5 mM Ce(NO$_3$)$_3$, (2) 5 mM Ce(NO$_3$)$_3$ + 1.5 mM Al(NO$_3$)$_3$, (3) 5 mM Ce(NO$_3$)$_3$ + 1.5 mM Al(NO$_3$)$_3$ + 1 mM Ca(OH)$_2$.

calcium hydroxide addition, microcracks are still visible in the surface and cross section images. However, the width of cracks became smaller as shown in Figures 2a(2) and 2b(2). With addition of 1.5 mM Al(NO$_3$)$_3$, the coating appears to be smooth and dense and to cover the surface of the substrate completely without microcracks. However, the surface is containing some of agglomerated particles as shown in Figure 2a(3). The cross section of the film (Figure 2b(3)) was denser and with no cracks or pores.

The major anodic reaction is the dissolution of magnesium that is likely to occur at anodic sites in the surface immediately upon immersion in the treatment solution.

$$Mg = Mg^{2+} + 2e^- \quad (1)$$

The cathodic reactions begin immediately when the Mg specimen is immersed in the treatment solution. Essentially, this results in the deposit of the hydrated cerium oxides on the cathodic sites at the surface owing to a local pH increase: In the lower pH range, Ce^{III} is the more stable form

$$2H_2O + 2e^- = 2OH^- + H_2 \quad (2)$$

$$Ce^{3+} + 3OH^- = Ce(OH)_3 \quad (3)$$

$$2Ce(OH)_3 = Ce_2O_3 + 3H_2O \quad (4)$$
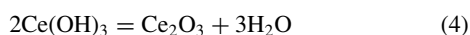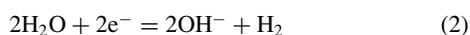
At higher pH values, Ce^{IV} becomes the more stable form, Ce^{III} may be oxidized to Ce^{IV} and the following reaction is occur

$$Ce_2O_3 + O_2 = 2CeO_2 \quad (5)$$
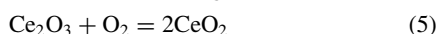
Figure 3 shows the XRD analysis of the conversion coating film. After conversion treatment in 5 mM Ce(NO$_3$)$_3$ solution (pH 4.5), the main peaks were for Mg, Mg(OH)$_2$, Ce$_2$O$_3$, and Ce(OH)$_3$ as shown in Figure 3(1). With addition of 1 mM Ca(OH)$_2$ (pH 6.5), Mg(OH)$_2$ peak became higher, CeO$_2$ peak was detected as shown in Figure 3(2) and Ce^{III} oxidized to Ce^{IV} according to eq. 5. In the solution; 5 mM Ce(NO$_3$)$_3$ + 1.5 mM Al(NO$_3$)$_3$ + 1 mM Ca(OH)$_2$, the peak of Mg(OH)$_2$ has the highest intensity as shown in Figure 3(3). Therefore, the enhancement of the anticorrosion property was induced by the convertion of the more soluble Ce^{III} to Ce^{IV} precipitates.

Figure 4 compared the anodic polarization curves before (nontreated) and after 15 min treatment in (1) 5 mM Ce(NO$_3$)$_3$, (2) 5 mM Ce(NO$_3$)$_3$ + 1.5 mM Al(NO$_3$)$_3$, and (3) 5 mM Ce(NO$_3$)$_3$ + 1.5 mM Al(NO$_3$)$_3$ + 1 mM Ca(OH)$_2$. The anticorrosion property of conversion coating films is better than nontreated specimen. The corrosion properties of conversion coating was enhanced with Ca(OH)$_2$ additions (Figure 4(2)). The role of Ca cation is still controversial, and more investigations are being carried out now to give clear explanation. With addition of 1.5 mM
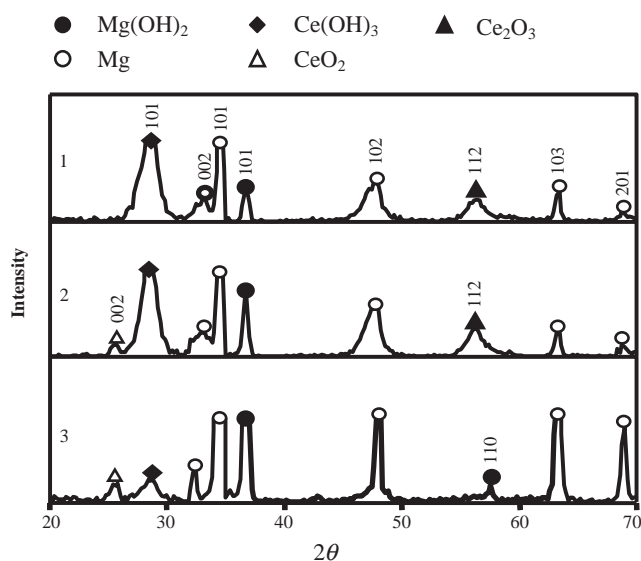
Figure 3. XRD patterns of the coating after 15 min treatment (1) 5 mM Ce(NO$_3$)$_3$, (2) 5 mM Ce(NO$_3$)$_3$ + 1.5 mM Al(NO$_3$)$_3$, (3) 5 mM Ce(NO$_3$)$_3$ + 1.5 mM Al(NO$_3$)$_3$ + 1 mM Ca(OH)$_2$.
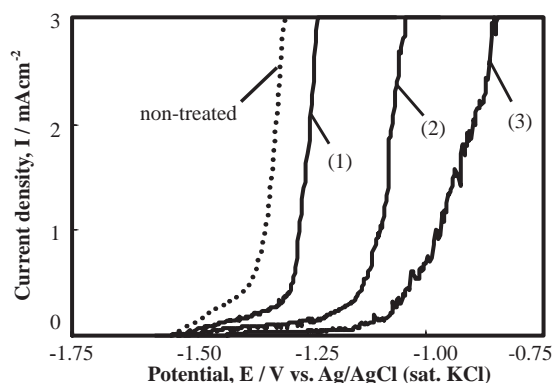
Figure 4. The anodic polarization curves before (nontreated) and after 15 min treatment in (1) 5 mM Ce(NO$_3$)$_3$, (2) 5 mM Ce(NO$_3$)$_3$ + 1.5 mM Al(NO$_3$)$_3$, (3) 5 mM Ce(NO$_3$)$_3$ + 1.5 mM Al(NO$_3$)$_3$ + 1 mM Ca(OH)$_2$.

Al(NO$_3$)$_3$ and 1 mM Ca(OH)$_2$ to cerium-based solution, the best corrosion resistance was observed as shown in Figure 4(3).

As described above the corrosion property of conversion coating is improved with increasing of the immersion time. Addition of Ca(OH)$_2$ and Al(NO$_3$)$_3$ to cerium-based solution enhanced the anticorrosion property of the film.

References
1　E. F. Emley, *Principle of Magnesium Technology*, Pergamon Press, London, **1966**.
2　Y. Mizutani, S. J. Kim, R. Ichino, M. Okido, *Surf. Coat. Technol.* **2003**, *169*, 143.
3　J. E. Gray, B. Luan, *J. Alloys Compd.* **2002**, *336*, 88.
4　S.-J. Kim, Y. Zhou, R. Ichino, M. Okido, S. Tanikawa, *Metals Mater. Int.* **2003**, *9-2*, 207.
5　S.-J. Kim, M. Okido, *Bull. Korean Chem. Soc.* **2003**, *24*, 8975.
6　M. Dabala, K. Brunelli, E. Napolitani, M. Magrini, *Surf. Coat. Technol.* **2003**, *172*, 227.
7　M. Dabala, L. Armelao, A. Buchberger, I. Calliari, *Appl. Surf. Sci.* **2001**, *172*, 312.
8　A. Froats, T. K. Aune, D. Hawke, W. Unsworth, J. Hillis, *Metals Handbook*, 9th ed., ASM Int., **1987**, Vol. 13, p. 740.
9　C. S. Lin, S. K. Fang, *J. Electrochem. Soc.* **2005**, *B54*, 152.
10　H. Ardelean, C. Fiaud, P. Marcus, *Mater. Corrosion* **2001**, *52*, 889.
11　K. Hirai, H. Somekawa, Y. Takigawa, K. Higashi, *Mater. Sci. Eng. A* **2005**, *403*, 276.
12　B. S. You, W. W. Park, I. S. Chung, *Scripta Mater.* **2000**, *42*, 1089.